이학석사 학위논문

암 세포주의 G2, M기에서 과량의 중심립 생성에 관한 연구

Studies on the supernumerary centriole assembly at G2 and M phases in cancer cell lines

2022년 8월

서울대학교 대학원

생명과학부

김 명 세

암 세포주의 G2, M기에서 과량의 중심립 생성에 관한 연구

Studies on the supernumerary centriole assembly at G2 and M phases in cancer cell lines

지도교수 이 건 수

이 논문을 이학석사 학위논문으로 제출함

2022년 6월

서울대학교 대학원
생명과학부
김 명 세

김명세의 이학석사 학위논문을 인준함

2022년 6월

위 원 장 _____(인)
부위원장 _____(인)
위 원 _____(인)

Studies on the supernumerary centriole assembly at G2 and M phases in cancer cell lines

A dissertation submitted in partial
fulfillment of the requirement
for the degree of

MASTER OF PHILOSOPHY

to the Faculty of
School of Biological Sciences
at
Seoul National University
by

Myungse Kim

Date Approved:
June, 2022

_____

_____

_____

ABSTRACT

Studies on the supernumerary centriole assembly at G2 and M phases in cancer cell lines

Myungse Kim

School of Biological Science

The Graduate School

Seoul National University

Centrioles duplicate and segregate in close link to the cell cycle. At S phase, a daughter centriole assembles at the proximal end of the pre-existing centriole. At end of mitosis, two centriole pairs separate into each daughter cell. The centriole number must be tightly regulated, otherwise abnormal spindles form, resulting in mitotic catastrophe and aneuploidy. Nonetheless, cancer cells frequently include supernumerary centrioles, bearing such disadvantages. In my thesis work, I investigated how supernumerary centrioles are formed in selected cancer cell lines. I conducted sequential

immunostaining to count centriole numbers at specific cell cycle stages in 16 cancer cell lines. The results showed that the number of supernumerary centrioles significantly increased at G2 and M phases in 4 cancer cell lines, such as MDA-MB-157, DU145, SKBR3, and RD. However, I was not able to detect the S phase centriole amplification among the cancer cell lines I examined. I also observed precocious centriole separation at M phase in MDA-MB-157 and RD which have supernumerary centrioles at M phase. Based on the results, I propose that the M phase centriole amplification may occur in selected cancer cell lines.

Key Words: Supernumerary centrioles, Centrosome, Centriole separation, PCM, Cancer

Student Number: 2020-20171

CONTENTS

LIST OF FIGURES

INTRODUCTION

Centrosomes function as a microtubule organizing center (MTOC) in animal cells. The centrosome helps the cell to form a bipolar spindle in cell division so that chromosome segregation could be done right (Conduit et al., 2015). When cells get into the resting phase called G0, the centrosome becomes the basal body to make primary cilia which function as signal receptors (Avidor-Reiss and Gopalakrishnan, 2013).

The microstructure of the centrosome has been revealed with the development of electron microscopy since the 1950s. The centrosome consists of a centriole and pericentriolar material (PCM) (Stearns et al., 2004). PCM is a group of proteins that forms an amorphous structure that surrounds two centrioles. Pericentrin (PCNT), CEP215, CEP192, and CEP152 were examples of PCM proteins. (Woodruff et al., 2014). The centriole is a cylindrical structure made up of nine sets of microtubule triplets.

Centriole duplicates once and only once in the S phase from a pre-existing centriole, the mother centriole (Nigg and Holland, 2018). The daughter centriole grows from a structure called a cartwheel which is made perpendicular to the mother centriole which is promoted by centriole duplication master regulator PLK4 (Habedanck et al., 2005). The orthogonal position of these centrioles blocks another formation of centrioles even though the level of PLK4 maintains high during the M phase (Holland et al., 2010). Their positions are maintained until mitotic exit due to surrounding PCM (Cabral et al., 2013; Seo et al., 2015). In mitosis, centriole separate from each other which is called centriole disengagement. When the cell exits the M phase, associated centrioles become

separated which gives an opportunity for centriole duplication at the next cell cycle called licensing of centriole duplication (Nigg, 2007). As a component of the centrosome, the centriole number must be strictly regulated. Numeral defect in centriole number, such as centrosome amplification causes various problems in cell. For example, asymmetric division, aneuploidy, problems in polarity, signaling, and microtubules (Godinho and Pellman, 2014).

After finding centrosome amplification is caused by an absence of p53, many reported supernumerary centrioles in cancer (Fukasawa et al., 1996; Wong et al., 2015; Marteil et al., 2018; Sankaran et al., 2019; Adams et al., 2021) Correlation between supernumerary centriole and caner has been mentioned for a long time. The supernumerary centriole is a common characteristic of cancer and it is reported supernumerary centriole induces tumorigenesis by chromosome instability and wrong cell division (D' Assoro et al., 2002; Fukasawa 2005; Godinho and Pellman, 2014).

Understanding the mechanistic generation of supernumerary centrioles is important because it can be used for cancer therapy. Supernumerary centrioles are made in many ways. (1) cytokinesis failure (Davoli and de Lange, 2011; Holland and Cleveland, 2009) (2) overexpression of PLK4 (Kleylein-Sohn et al., 2007) In these cases, newly formed centrioles are made in the S phase. But in a recent study, in artificially manipulated PCM disintegrated cells, centrioles can also be made in the M phase, and this happens in cells from which the mother and daughter centrioles are separated early (Kim et al., 2019; Jung and Rhee 2021). Extra centrioles are deleterious since they make multipolar spindle poles during mitosis, Nevertheless, supernumerary centrioles are frequently detected in cancer cells (Fukasawa et al., 2005; Wong et al., 2015; Marteil et al., 2018; Sankaran et al., 2019; Adams et al., 2021). During my master's training period, I investigated

how supernumerary centrioles are generated in cell lines that are derived from cancer tissues.

MATERAILS AND METHODS

Cell culture

MDA-MB-157, MDA-MB-468, MDA-MB-231, and MCF7 were kindly provided by Professors Won Shik Han from Seoul National University. BT549, Hs578T from Sujae Lee. SKBR3, BT20, HCC1937, HCC1954, RD, H23, PANC-1, DU145, PC3, and HCT116 cell lines were obtained from Korean Cell Line Bank. hTERT-RPE1, HeLa, PLK4 overexpressing HeLa, MDA-MB-468, MDA-MB-231, MCF7, Hs578T, RD, PANC-1, and HCT116 cells were cultured in DMEM (Welgene, LM001-05) supplemented with 10 % FBS (Welgene, S101-01) and antibiotics (Invivogen, ANT-MPT). MDA-MB-157, BT549, SKBR3, BT20, HCC1954, HCC1937, H23, DU145, and PC3 cells were cultured in RPMI1640 (Welgene, LM011-01) supplemented with 10 % FBS and antibiotics. *TP53;PCNT;CEP215* triple knockout cell line was generated in the Flp-InT-Rex HeLa cells. TKO HeLa cells were cultured in DMEM supplemented with 10% Tet-system approved FBS (Taraka, 630017) to complete the TKO (Jung and Rhee, 2021). PLK4 overexpressing HeLa cells were treated with doxycycline(100ng/ml) for 24 h to induce ectopic expression of PLK4.

Cell synchronization and Drug treatments

To acquire cells for each cell cycle, cells were treated with 2mM thymidine for 24 h and 5μM RO3306 for 8 h then fixed at a specific timepoint. S and G2 phase cells were got from right after thymidine and RO3306 treatment respectively. After thymidine-RO3306 cell cycle arrest, cells were washed twice with warm PBS and

then cultured in fresh media. M phase cells got from 30 min after release and G1 cells from 4 h after release.

Antibodies

Antibodies for CEP135 (ICC 1:2000) (Kim et al., 2008) and CP110 (ICC 1:1000) (Kim et al., 2008) were described previously. Centrin-2 (ICC 1:1000) (Millipore, 04-1624), CyclinB1 (ICC 1:50) (Santacruz, Sc-245), BrdU (ICC 1:1000) (Sigma, 59-14-3) were purchased. Alexa 488, 555 (ICC 1:1000) (Invitrogen) were used as secondary antibodies for Immunocytochemistry analyses.

Immunofluorescence microscopy

In order to detect S phase cells, cells were incubated with BrdU(20mM) for 1h. the BrdU incorporated cells were fixed with cold methanol for 10 min at 4℃, washed 3 times with cold PBS, then treated with PBST (0.1% Triton X-100 in PBS) for 10 min and blocked with the blocking solution (3% bovine serum albumin, and 0.3% Triton X-100 in PBS) for 30 min. The samples were incubated with primary antibodies except for BrdU for 1 h, washed with 0.1% PBST 3 times, incubated with secondary antibodies for 30 minutes, washed with 0.1% PBST 3 times, post-fixed with 4% paraformaldehyde for 8 h in 4℃. The cells are washed 3 times with PBS, then treated with PBST again. The cells were denatured by pre-heated 37℃ 2N HCL, 10 min of stabilization by Sodium Borate buffer (1M, pH 8.5), and washed with PBS 3 times. The samples are re-blocked with a blocking solution for 30 min. The samples were incubated with primary BrdU antibody for 1 h, washed with 0.1% PBST, and incubated with secondary antibody

for 30 minutes. The samples were treated with 4,6-diamidino-2-phenylindole (DAPI) solution for up to 3 minutes. The cover glasses were mounted on a slide glass with ProLong Gold antifade reagent (Life Technologies, P36930). Images were observed with fluorescence microscopes with a digital camera (Olympus IX51) equipped with QImaging 336 QICAM Fast 1394 and processed in PVCAM (Teledyne). PVCAM and ImageJ 1.53k (National Institutes of Health) were used for image processing.

Fluorescence-activated cell sorting

To prepare cells for FACS analysis, cultured cancer cells were harvested with 0.25% (w/ v) Trypsin/EDTA (Welgene, LS015-01). For fixation, cold 70% ethanol was added to the sample while vortexing and stored at 4℃ for a minimum of 10 minutes. Cells were washed three times in PBS. Propidium iodide (PI) with RNase and EDTA (7.5pH) was used for DNA staining. 10000 cells were counted for each sample to draw the propidium iodide-DNA histogram plot. FACS data was collected in FACS CANTO 2 (BD Biosciences).

Statistical analysis

For statistical analyses, experiments were independently performed three times. To calculate P values, a one-way analysis of variant (ANOVA) was performed in Prism 5 (GraphPad Software). In the case of ANOVA, Tukey's multiple comparisons test was performed to compare with the previous cycle stage. All measured displayed with column bar graph, vertical in Prism 5.

RESULTS

Presence of supernumerary centrioles in the cancer cell lines

As centriole amplification is a common characteristic of cancer cells (Shin and Rhee, 2021). I selected 16 cancer lines and examined the presence of supernumerary centrioles (Table 1). As controls, I used human retinal pigment epithelial-1 (RPE-1), and HeLa cells with overexpressing PLK4 (HeLa PLK4 OE) and *TP53;PCNT;CEP215* triple knockout (Hela TKO). RPE-1 included supernumerary centrioles in 3% of the cell population (Figure 1). Supernumerary centrioles were also observed in 1% of the HeLa cells and this number increased by 53% in the PLK4-overexpressing HeLa cells (Figure 1). The triple KO cells also included supernumerary centrioles to 5% (Figure 1). In these conditions, I observed supernumerary centrioles at 1.3-8% of the cancer cell line population (Figure 1). Most cancer cell lines include more supernumerary centrioles than the control cells. However, these numbers are somewhat smaller than previously reported (Brodie and Henderson, 2012; Wong et al., 2015; Rhys et al., 2018; Arnandis et al., 2018; Marteli et al 2018; Adams et al., 2021). In this study I used two centriole markers, centrin-2(CETN2) and CP110, when the two marker signals are overlapped, I counted that as centriole (Marteli et al., 2018). This conserved way to count the number of centrioles may reduce the counting values smaller than the other reports. In fact, the centrosome amplification percentages of the same cell lines fluctuate among the reports, suggesting that the error ranges in centriole number counting should be quite large (Wong et al., 2015; Rhys et al., 2018; Marteli et al 2018).

Determination of the cell cycle stage and centriole number in individual cells

To count the centriole numbers at specific cell cycle stages in asynchronous cell populations, I performed a sequential immunostaining using the BrdU, cyclin B1, centrin2, and CP110 antibodies (Figure 2a). Cells were cultured under optical conditions. Forty-eight hours after seeding, the cells were treated with BrdU for 1 h and fixed for immunostaining with the antibodies specific to cyclin B1, centrin2, and CP110. After the immunostaining, the cells were fixed again with 4% paraformaldehyde for 24 h, treated with 2N HCl for 30 min at 37°C to denature DNA, and then subjected to second immunostaining with the BrdU antibody. BrdU is a S phase marker while cyclin B1 is a G2 phase marker (Gasparri et al., 2006; Figure 2b). The G1 phase cells were not immunostained with both the antibodies while the M phase cells were distinguished by their unique DAPI morphology (data not shown). CETN2 and CP110 were used for centriole markers (Marteli et al., 2018). I counted centrioles only when both the centrin2 and CP110 signals overlapped (Figure 2c). I counted all the cells in a microscope field to reduce an error generated by selected cell counting. However, I looked for the M phase cells were searched in the microscope fields, since they were presented in low proportions. I counted about 20 mitotic cells per each experiment. After repeating the experiments 3 times, I statistically analyzed the data and presented in Figure 3.

The results showed that most of the cancer cell lines had 1,2 centrioles in the G1 phase and 3,4 centrioles in S, G2, and M phases (Figure 3, Table2). In addition, selected cell lines include supernumerary centrioles at specific cell cycle stages. For example, MDA-MB-157, DU145, SKBR3, and RD cells had

supernumerary centrioles at M phase (Figure 3). I also observed that most cancer cell lines included 3,4 centrioles at G1 phase, but it is not statistically significant (Figure 3). To my surprise, supernumerary centrioles were not prominent at S phase of most cancer cell lines (Figure 3). It is quite surprising since centriole assembly occurs at S phase (Nigg, 2007; Wang et al., 2014).

I determined the centriole numbers in synchronized populations of the selected cancer cells. I used thymidine and RO3306 to arrest the cells at S and G2 phases, respectively. After the cells were seeded on coverslips, they were subjected to thymidine-RO3306 cell cycle synchronization (Figure 4a). The cells were fixed at indicated time points for S, G2, M, and G1 phase cells. Cell synchronization was confirmed with the FACS analysis (Figure 4b).

Centriole numbers of the synchronized Hela FRT/TO, PLK4 overexpression Hela, TKO Hela, MDA-MB-157, and RD were counted by sequential immunostaining (Figure 4c, Table 3). Most of the G1 Hela cells include 1,2 centrioles, whereas most of the S, G2, and M phase HeLa cells included 3,4 centrioles (Figure 4c). This number is consistent with those in the asynchronous populations in Figure 3. Likewise, supernumerary centrioles were observed in all cell cycle stages of the HeLa cells overexpressing PLK4 (Figure 4c). In the case of the triple KO HeLa cells, the supernumerary centriole population was significant at G2 and M phases (Figure 4c). In such conditions, I observed the presence of supernumerary centrioles at M phase of the MDA-MB-157 and RD cell lines. This is the first evidence that centriole amplification occurs at M phase in selected cancer cell lines.

Precocious centriole separation observed in M phase centriole amplifying cancer cell lines

To examine the mechanism for centriole amplification at G2 and M phases, I immunostained the M phase cells of Hela FRT/TO, PLK4 overexpression Hela, TKO Hela, MDA-MB-157, and RD with the antibodies specific to centrin-2 and CEP135. The CETN2 and CEP135 coimmunostaining is widely used to determine centriole disengagement (Tsou et al., 2006, 2009; Lee et al., 2012). The ratio of CETN2 to CEP135 is 2 when centrioles were associated, and the ratio is 1 when centrioles separate each other (Figure 5a).

A centriole pair should be associated within the spindle pole during the M phase (Figure 5b, c). When specific PCM protein genes are deleted, the centrioles may be precociously separated at M phase and eventually amplify at M phase (Figure 5b, c; Kim et al., 2019; Jung and Rhee, 2021). I observed M phase centrioles in selected cancer cell lines. The results showed 36 and 33 % of mitotic MDA-MD-157 and RD cells had separated centrioles, respectively (Figure 5b, c). These results suggest that M phase centriole assembly in MDA-MD-157 and RD might be resulted from precocious centriole separation.

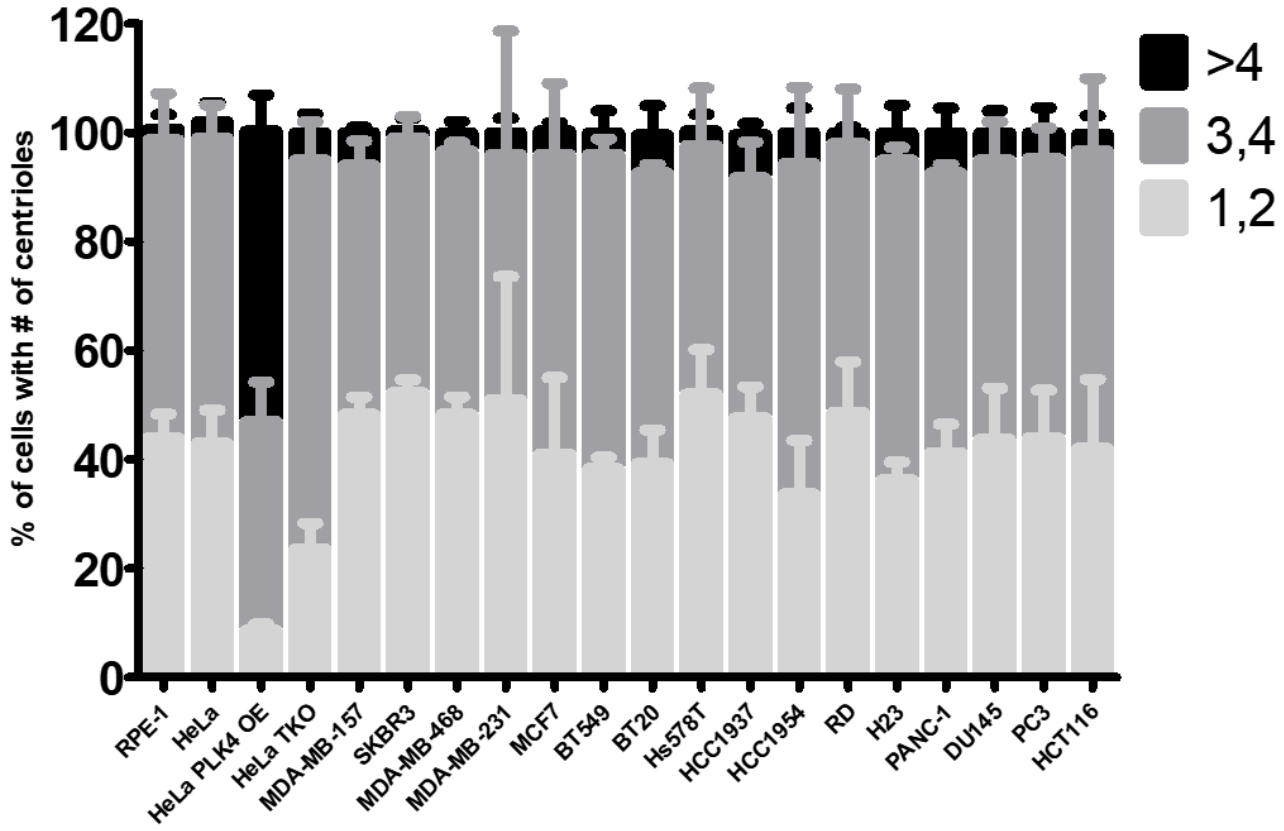

Figure 1. Centriole counting in the cancer cell lines

The cancer cells were coimmunostained with the antibodies specific to centrin-2 and CP110, and their centriole numbers were counted. The cell lines were originated from breast cancer (MDA-MB-157, Hs578T, MDA-MB-468, MDA-MB-231, MCF7, BT549, BT20, HCC1937, HCC1954, and SKBR3), pancreatic cancer (PANC-1), colon cancer (HCT116), prostate cancer (DU145 and PC3), lung cancer (H23), and muscle cancer (RD). I used RPE1 and the PLK4-overexpressing and triple KO HeLa cells as controls. Greater than 70 cells per experimental group were counted in three independent experiments.

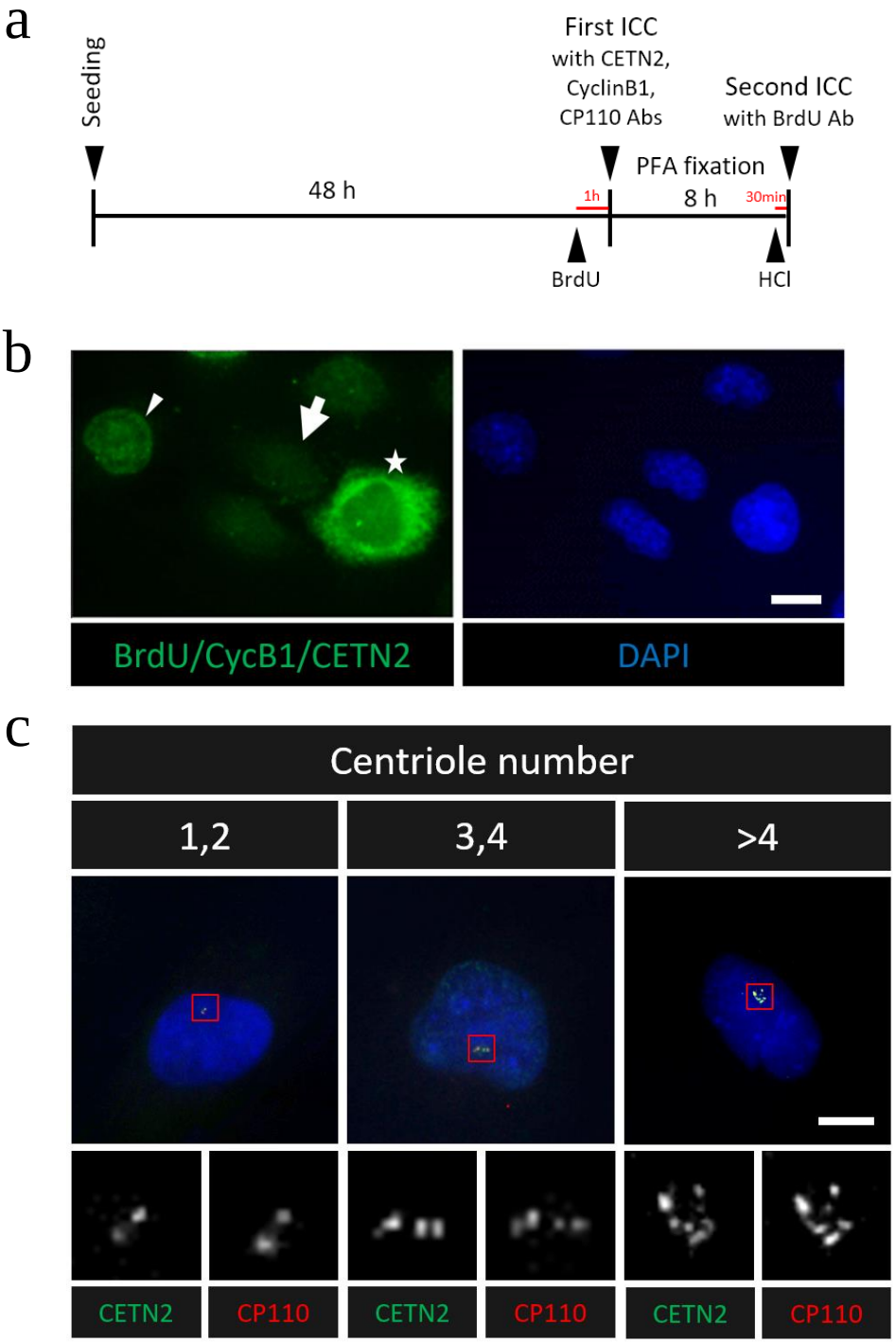

Figure 2. Sequential coimmunostaining analysis for determination of the centriole numbers at specific cell cycle stages

(a) Schematic illustration of the sequential coimmunostaining analysis for determination of the cell cycle stages and centriole numbers of individual cells. (b) Hela cells were coimmunostained with the antibodies specific to BrdU (green), cyclin B1 (green), and centrin2 (green). Nuclei were stained with DAPI (blue). Arrowhead, arrow, and asterisk represent cells at S (BrdU-positive), G1 (BrdU-negative, cyclin B1-negative) and G2 (cyclin B1-positive) phases, respectively. Scale bar, 10 μm (c) The number of centrioles were counted with the signals of centrin-2 (green) and CP110(red). Nuclei were stained with DAPI (blue). Scale bar, 10 μm

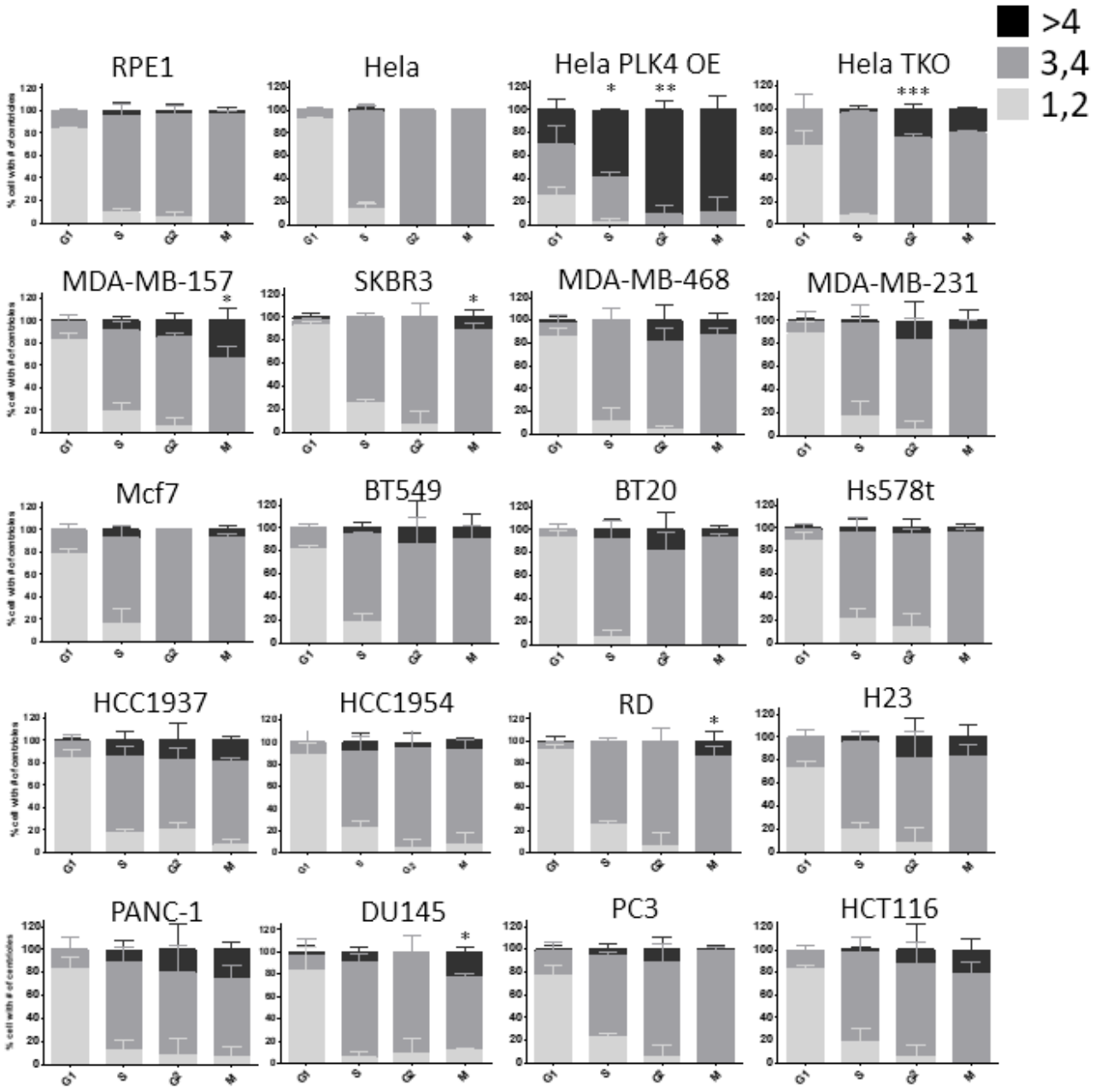

Figure 3. Determination of the number of centrioles at specific cell cycle stages of the cancer cells

The number of centrioles at specific cell cycle stages are counted with the sequential coimmunostaining method. Greater than 90 cells per experimental group were counted in three independent experiments. The statistical analysis was performed with one-way ANOVA and Tukey's multiple comparisons test in >4 centrioles number compared to the previous phase. (*, $P<0.05$, **, $P<0.01$, ***, $P<0.001$)

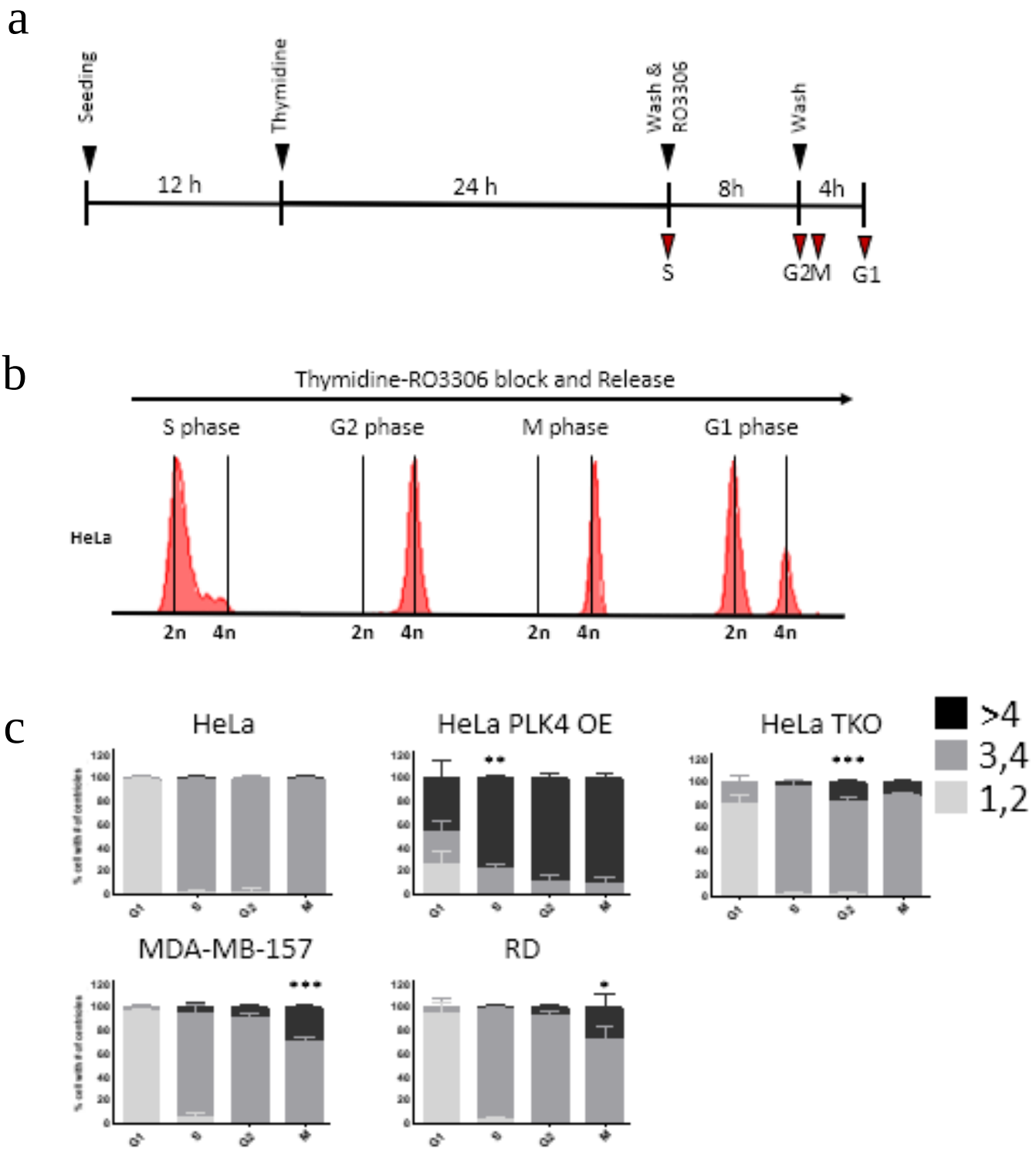

Figure 4. Determination of the number of centrioles in synchronous populations of the cancer cells

(a) Synchronized population at specific cell cycle stages were obtained with sequential treatment of thymidine and RO3306. (b) Representative FACS analysis of HeLa to confirm synchronization of the cell population. (c) The cells were sequentially coimmunostained with BrdU, cyclin B1, centrin2 and CP110 to determine centriole numbers at specific cell cycle stages. Greater than 80 cells per experimental group were counted in three independent experiments. The statistical analysis was performed with one-way ANOVA and Tukey's multiple comparisons test in >4 centrioles number compared to the previous phase (*, $P<0.05$, **, $P<0.01$, ***, $P<0.001$).

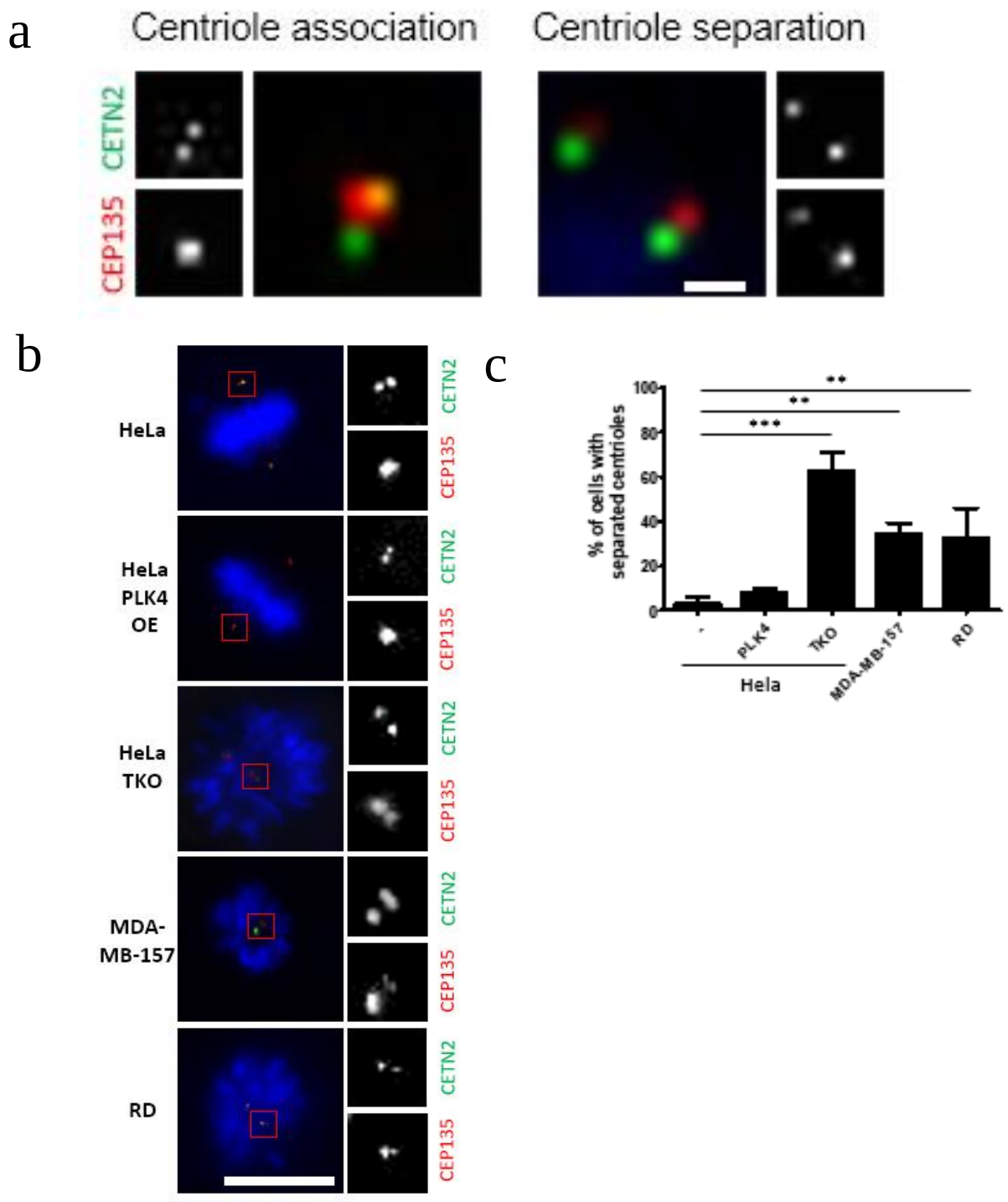

Figure 5. Premature centriole separation at M phase in the cancer cell lines

(a) HeLa cells were subjected to coimmunostaining analyses with antibodies specific to centrin2 (CETN2, green) and CEP135 (red). Scale bar, 1 μm. CETN2 and CEP135 signal ratio 2:1 represents centriole association and 1:1 represents centriole separation. (b) Representative images of centrioles at M phase of MDA-MB-157, RD, DU145, and the HeLa control cells. Nuclei were stained with DAPI (blue). Scale bar, 10 μm (c) The number of cells with separated centrioles at M phase was counted and statistically analyzed. Greater than 30 cells per experimental group were counted in three independent experiments. The statistical analysis was performed with one-way ANOVA and Tukey's multiple comparisons test in >4 centrioles number compared to the previous phase (**, $P<0.01$, ***, $P<0.001$).

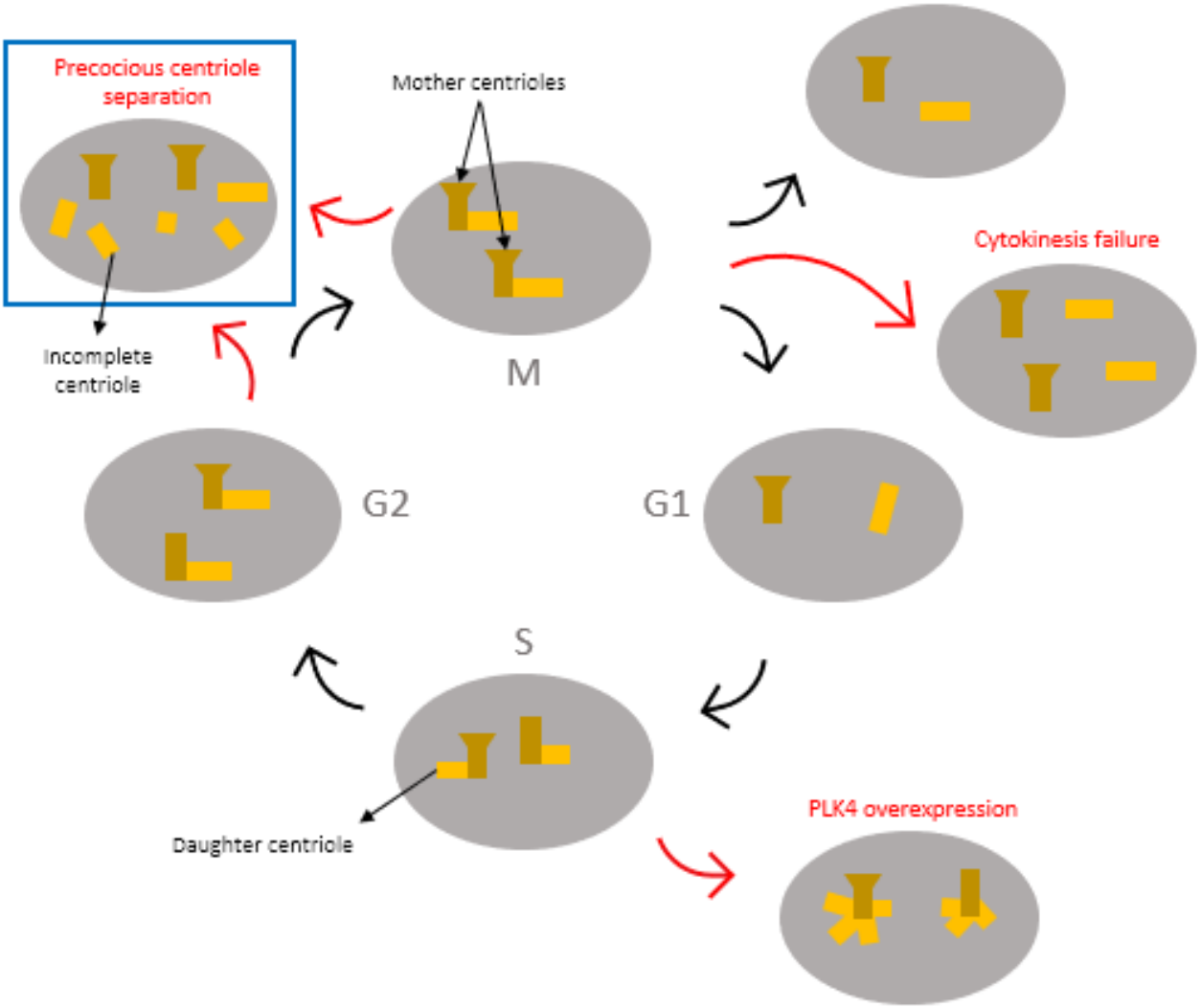

Figure 6. Generation of supernumerary centrioles in cancer cells
Centrioles duplicate at S phase and segregate at M phase during the normal cell cycle. It was previously reported that supernumerary centrioles are generated in several ways, such as PLK4 overexpression, precious centriole separation and cytokinesis failure. In this thesis, I propose that precocious centriole separation may be installed at selected cancer cell lines for constant generation of supernumerary centrioles during the cell cycle.

Table 1. Centriole amplification in various cancer cell lines
List of cancer cell lines that are reported to have supernumerary centrioles at M phase.

Cell line	organ	CA(%)	Reference
MDA-MB-157	Breast	-	-
SKBR3	Breast	25	Patel et al., 2018
MDA-MB-468	Breast	6	Rhys et al., 2018
MDA-MB-231	Breast	14.5	Marteli et al., 2018
Mcf7	Breast	5.2	Marteli et al., 2018
BT549	Breast	19	Wong et al., 2015
BT20	Breast	6	Rhys et al., 2018
Hs578t	Breast	32.6	Marteli et al., 2018
HCC1937	Breast	20	Brodie and Henderson, 2012
HCC1954	Breast	16	Amandis et al., 2018
RD	Muscle	22	Wong et al., 2015
H23	Lung	37.5	Marteli et al., 2018
PANC-1	Pancreas	54.8	Adams et al., 2021
DU145	Prostate	16.5	Marteli et al., 2018
PC3	Prostate	7.3	Marteli et al., 2018
HCT116	Colon	9	Wong et al., 2015

Table 2. The number and percentage of centrioles in asynchronous cancer cells with cell stage information

		1st trial (#(%))				2nd trial (#(%))				3rd trial (#(%))			
Cells	Stages	1,2	3,4	>4	Total	1,2	3,4	>4	Total	1,2	3,4	>4	Total
RPE-1	G1	18(81)	4(19)	0	22	42(84)	8(16)	0	50	36(84)	7(16)	0	43
	S	2(11)	16(89)	0	18	3(12)	19(76)	3(12)	25	3(6)	44(84)	0	47
	G2	1(10)	9(90)	0	10	1(6)	15(83)	2(11)	18	0	5(100)	0	5
	M	0	21(95)	1(5)	22	0	20(100)	0	20	0	22(96)	1(4)	23
HeLa	G1	20(91)	2(9)	0	22	29(91)	3(9)		32	26(93)	2(7)		28
	S	3(9)	28(99)	1(3)	32	3(12)	23(88)		26	7(19)	29(78)	1(3)	37
	G2		8(100)		8		10(100)		10		6(100)		6
	M		22(100)		22		18(100)		18		22(100)		22
HeLa PLK4 OE	G1	6(24)	12(48)	7(28)	25	5(33)	4(27)	6(40)	15	5(19)	15(58)	6(23)	26
	S		19(43)	25(57)	44	2(5)	16(36)	26(59)	44	1(20	17(40)	24(57)	42
	G2			5(100)	5		1(13)	7(88)	8		1(14)	6(86)	7
	M		4(25)	12(75)	16			19(100)	18		2(10)	18(90)	20
HeLa TKO	G1	19(79)	5(21)		24	11(55)	9(45)		20	15(71)	6(29)		21
	S	3(8)	33(87)	2(5)	38	4(9)	41(91)		45	3(6)	45(88)	3(6)	51
	G2		11(79)	3(21)	14		3(75)	1(25)	4		5(71)	2(29)	7
	M		18(78)	5(22)	23		17(81)	4(19)	21		19(79)	5(21)	24
MDA-MB-157	G1	40(78)	11(22)	0	51	32(89)	4(11)	0	36	45(83)	8(15)	1(2)	54
	S	6(14)	35(80(	3(7)	44	11(28)	25(64)	3(8)	39	5(16)	22(71)	4(13)	31
	G2	0	4(80)	1(20)	5	2(15)	10(77)	1(8)	13	0	5(83)	1(17)	6
	M	0	20(74)	7(26)	27	0	16(64)	9(36)	25	0	16(59)	11(41)	27
SKBR3	G1	28(93)	2(7)		30	24(96)	1(4)		25	24(89)	1(4)	2(7)	27
	S	10(24)	31(76)		41	12(29)	30(71)		42	6(24)	19(76)		25
	G2		5(100)		5	1(20)	4(80)	0	5		3(100)		3
	M		17(85)	3(15)	20		23(96)	1(4)	24		17(85)	3(15)	20
MDA-MB-468	G1	26(84)	3(10)	2(6)	31	33(94)	2(6)	0	35	30(81)	7(19)	0	37
	S	4(14)	25(86)	0	29	4(21)	15(79)	0	19	0	12(100)	0	12
	G2	0	2(67)	1(33)	3	1(5)	17(89)	1(5)	19	1(5)	15(79)	3(16)	19
	M	0	21(84)	4(16)	25	0	17(94)	1(6)	18	0	14(82)	3(18)	17
MDA-MB-231	G1	13(100)	0	0	13	18(86)	3(14)	0	21	30(81)	6(16)	1(3)	37
	S	2(15)	11(85)	0	13	1(6)	15(94)	0	16	9(30)	19(63)	2(7)	30
	G2	0	1(100)	0	1	1(14)	5(71)	1(14)	7	0	6(67)	3(33)	9
	M	0	17(94)	1(6)	18	0	19(100)	0	19	0	14(82)	3(18)	17
Mcf7	G1	16(84)	3(16)	0	19	21(75)	7(25)	0	28	17(77)	5(23)	0	22
	S	4(29)	9(64)	1(7)	14	1(3)	19(87)	4(10)	39	8(18)	34(77)	2(5)	44
	G2	0	2(100)		2	0	5(100)	0	5	0	4(100)	0	4
	M	0	18(90)	2(10)	20	0	19(95)	1(5)	20	0	19(95)	1(5)	20
BT549	G1	35(78)	10(22)	0	45	18(82)	4(18)	0	22	16(84)	3(16)	0	19
	S	5(13)	31(78)	4(10)	40	6(16)	29(76)	3(8)	38	12(26)	35(74)	0	47
	G2	0	11(100)	0	11	0	3(60	2(40)	5	0	6(100)	0	6
	M	0	24(100)	0	24	0	19(95)	1(5)	20	0	18(78)	5(22)	23
BT20	G1	20(100)	0	0	20	26(90)	3(10)		29	31(82)	7(18)		38
	S	2(7)	24(89)	1(4)	27	3(12)	18(69)	5(19)	26		17(100)		17
	G2		11(65)	6(35)	17		18(90)	2(10)	20		11(92)	1(8)	12
	M	0	21(95)	1(5)	22		21(95)	1(5)	22		16(89)	2(11)	18
Hs578T	G1	26(93)	2(7)	0	28	34(94)	2(6)	0	36	23(82)	4(14)	1(4)	28
	S	4(25)	10(63)	2(13)	16	10(26)	29(74)	0	39	3(11)	25(89)	0	28
	G2	0	6(86)	1(14)	7	2(20)	8(80)	0	10	1(20)	4(80)	0	5
	M	0	18(100)	0	18	0	17(94)	1(6)	18	0	14(93)	1(7)	15
HCC1937	G1	22(92)	2(8)		24	25(83)	5(17)		30	29(78)	7(19)	1(3)	37
	S	6(17)	27(77)	2(6)	35	5(17)	20(67)	5(17)	30	4(20)	12(60)	4(20)	20
	G2	1(14)	4(57)	2(29)	7	2(22)	5(56)	2(22)	9	2(25)	6(75)		8
	M		14(78)	4(22)	18	2(11)	14(74)	3(16)	19	2(8)	17(71)	5(21)	24
HCC1954	G1	7(78)	2(22)		9	15(88)	2(12)		17	8(100)			8
	S	14(26)	26(67)	4(7)	54	8(26)	18(58)	5(16)	31	9(17)	43(83)		52
	G2		9(100)		9		3(100)		3	1(14)	5(71)	1(14)	7
	M	3(15)	15(75)	2(10)	20		17(94)	1(6)	18		17(94)	1(6)	18
RD	G1	33(94)	2(6)	0	35	15(60)	1(4)	1(4)	25	22(81)	1(4)	1(4)	27
	S	3(7)	16(39)		41	6(14)	25(60)		42	9(36)	24(96)		25
	G2		4(80)	1(20)	5		2(40)		5		11(100)		18
	M		16(80)	4(20)	20		17(85)	3(15)	20		19(95)	1(5)	20
H23	G1	16(80)	4(20)		20	12(71)	5(29)		17	11(69)	5(31)		16
	S	4(14)	25(86)		29	8(21)	28(74)	2(5)	38	8(24)	23(68)	3(9)	34
	G2		1(100)		1		2(67)	1(33)	3	3(23)	7(54)	3(23)	13
	M		15(75)	5(25)	20		16(80)	4(20)	20		21(95)	1(5)	22
PANC-1	G1	18(72)	7(28)	0	25	27(84)	5(16)	0	32	26(93)	2(7)		28
	S	5(16)	20(65)	6(19)	31	4(19)	16(76)	1(5)	21	1(3)	28(90)	2(6)	31
	G2	4(24)	10(59)	3(18)	17	0	11(100)	0	11		4(57)	3(43)	7
	M	3(17)	10(56)	6(33)	18	1(5)	17(77)	4(18)	22		15(71)	6(29)	21
DU145	G1	14(61)	7(30)	2(9)	23	33(94)	2(6)		35	32(97)	1(3)		33
	S		15(88)	2(12)	17	3(11)	21(78)	3(11)	27	2(6)	28(90)	1(3)	31
	G2	2(25)	6(75)		8		8(100)		8		8(100)		8
	M	2(11)	12(67)	4(22)	18	3(14)	15(68)	4(18)	22	2(11)	12(63)	5(26)	19
PC3	G1	15(71)	6(29)		21	25(86)	4(14)		29	15(75)	4(20)	1(5)	20
	S	5(24)	15(71)	1(5)	21	6(26)	17(74)		23	6(21)	20(69)	3(10)	29
	G2		9(82)	2(18)	11		5(100)		5	1(17)	4(67)	1(17)	6
	M		20(100)		20		21(95)	1(5)	22		20(100)		20
HCT116	G1	17(81)	4(19)		21	25(81)	6(19)		31	27(87)	4(13)		31
	S	2(5)	38(93)	1(2)	41	5(19)	21(81)		26	8(30)	18(67)	1(4)	27
	G2		4(100)		4		5(63)	3(38)	8	2(17)	10(83)		12
	M		15(71)	6(29)	21		19(76)	6(24)	25		18(90)	2(10)	20

Table 3. The number and percentage of centrioles in synchronous cancer cells

		1st trial (#(%))				2nd trial (#(%))				3rd trial (#(%))			
Cells	**Stages**	**1,2**	**3,4**	**>4**	**Total**	**1,2**	**3,4**	**>4**	**Total**	**1,2**	**3,4**	**>4**	**Total**
Hela FRT/TO	G1	21(100)			21	19(95)	1(5)		20	20(100)			20
	S		38(97)	1(3)	39		20(100)		20	1(5)	19(95)		20
	G2	1(3)	29(97)		31		20(100)		20	1(5)	19(95)		20
	M		20(100)		20		20(100)		20		19(95)	1(5)	20
Hela PLK4 OE	G1	4(20)	4(20)	12(60)	20	4(20)	7(35)	9(45)	20	8(40)	6(30)	6(30)	20
	S		5(25)	15(75)	20		4(20)	16(80)	20		5(24)	16(76)	21
	G2		4(17)	19(83)	23		2(10)	18(90)	20		2(10)	18(90)	20
	M		3(15)	17(85)	20		2(10)	18(90)	20		1(5)	19(95)	20
Hela TKO	G1	17(77)	5(23)		22	18(90)	2(10)		20	16(80)	4(20)		20
	S		19(95)	1(5)	20		20(100)	0	0	1(5)	18(90)	1(5)	20
	G2		17(85)	3(15)	20	1(5)	16(80)	3(15)	20		16(80)	4(20)	20
	M		18(90)	2(10)	20		17(85)	3(15)	20		18(90)	2(10)	20
MDA-MB-157	G1	19(95)	1(5)		20	19(95)	1(5)		20	20(100)			20
	S	2(10)	16(80)	2(10)	20	1(5)	19(95)	0	20	1(5)	18(90)	1(5)	20
	G2		18(90)	2(10)	20		19(95)	1(5)	20		18(90)	2(10)	20
	M		14(70)	6(30)	20		14(70)	6(30)	20		15(75)	5(25)	20
RD	G1	22(85)	4(15)		26	20(100)	0		20	20(100)			20
	S	1(4)	22(92)	1(4)	24	1(5)	19(95)		20	1(5)	19(95)		20
	G2		22(96)	1(4)	23		18(90)	2(10)	20		19(95)	1(5)	20
	M		19(83)	4(17)	23		12(60)	8(40)	20		15(75)	5(25)	20

DISCUSSION

In my thesis work, I investigated at which cell cycle stages centrioles are amplified in selected cancer cell lines. I detected supernumerary centrioles at G2 and M phases in 4 cancer cell lines among examined. These results suggest that extra centrioles may be formed at G2 and M phases in some cancer cells. It is surprising that I found none which had statistically significant number of extra centrioles at S phase among the cancer cell lines that I examined.

Multiple mechanisms have been proposed for centriole amplification during the cell cycle, including the M phase amplification mechanism (Shin and Rhee, 2021). It was previously reported that precocious centriole separation occurs, when PCM is scattered from the centrosome during G2 and M phases (Cabral et al., 2013; Seo et al., 2015). If the *PCNT* and *CEP215* genes were deleted, precocious centriole separation occurs and centriole amplification follows at M phase (Kim et al., 2019; Jung and Rhee, 2021; Figures 3, 4 and 6). In this study, I observed precocious centriole separation in MDA-MB-157 and RD cells (Figure 5). The same cell lines have supernumerary centrioles at M phase (Figure 3). These results suggest that defects in PCM assembly might be a causal event for supernumerary centrioles in selected cancer cell lines, such as MDA-MB-157 and RD cells.

It is surprising that the S phase centriole amplification has not been observed in my study (Figure 3). Many studies predicted that PLK4 overexpression may be the major mechanism for supernumerary centrioles, since PLK4 is a key kinase for centriole assembly at S phase. (Shinmura et al., 2014; Coelho et al., 2015; Sercin et al., 2016). I also observed the S phase centriole in

PLK4-overexpressing HeLa cells, but not in cancer cells that I examined (Figures 3, and 4). I imagine the following two possibilities. First, my experimental approach may have a technical shortage in detection of the S phase centriole amplification. Although S phase centriole amplification was detected in Hela PLK4 OE, this condition is quite different from natural cells as there are about 55% of cells have supernumerary centrioles (Figure 3; Kao et al., 2022). Indeed, cells such as PANC-1 and HCC1937 seem like make supernumerary centrioles at S phase though they are statistically not significant. A little bit of error in centriole number counting would have had an effect. Second, the S phase centriole amplification may be a rarer event than one expected. Supernumerary centrioles at S phase are reported only after manipulating the cells overexpress PLK4 (Stavenschi et al., 2017; Holland et al., 2012). But there is no evidence that this happens in natural cancer cell lines.

Supernumerary centriole can be formed in several ways. Cytokinesis failure is a well-known mechanism (Figure 6, McPherson et al., 2004; Fujiwara et al., 2005; Nishio et al. 2012). PLK4 overexpression also known to induce supernumerary centrioles (Figure 6, Kleylein-Sohn et al., 2007; Sabino et al., 2015) In this report, I propose that the PCM disintegration followed by precocious centriole separation may be another mechanism to generate supernumerary centrioles at G2 and M phase in selected cancer cell lines. (Figure 6).

REFERENCES

Conduit, P. T., Wainman, A., & Raff, J. W. (2015). Centrosome function and assembly in animal cells. *Nature reviews Molecular cell biology*, 16(10), 611-624.

Conduit, P. T., Wainman, A., & Raff, J. W. (2015). Centrosome function and assembly in animal cells. *Nature reviews Molecular cell biology*, *16*(10), 611-624.

Avidor-Reiss, T., & Gopalakrishnan, J. (2013). Building a centriole. *Current opinion in cell biology*, *25*(1), 72-77.

Stearns, T. (2004). The centrosome yields its secrets. *Nature Cell Biology*, *6*(1), 14-14.

Woodruff, J. B., Wueseke, O., & Hyman, A. A. (2014). Pericentriolar material structure and dynamics. *Philosophical Transactions of the Royal Society B: Biological Sciences*, *369*(1650), 20130459.

Nigg, E. A., & Holland, A. J. (2018). Once and only once: mechanisms of centriole duplication and their deregulation in disease. *Nature reviews Molecular cell biology*, *19*(5), 297-312.

Habedanck, R., Stierhof, Y. D., Wilkinson, C. J., & Nigg, E. A. (2005). The Polo kinase Plk4 functions in centriole duplication. *Nature cell biology*, *7*(11), 1140-1146.

Holland, A. J., Lan, W., Niessen, S., Hoover, H., & Cleveland, D. W. (2010). Polo-like kinase 4 kinase activity limits centrosome overduplication by autoregulating its own stability. *Journal of Cell Biology*, *188*(2), 191-198.

Cabral, G., Sans, S. S., Cowan, C. R., & Dammermann, A. (2013). Multiple mechanisms contribute to centriole separation in C. elegans. *Current biology*, *23*(14), 1380-1387.

Seo, M. Y., & Rhee, K. (2018). Caspase-mediated cleavage of the centrosomal proteins during apoptosis. *Cell death & disease*, *9*(5), 1-11.

Nigg, E. A. (2007). Centrosome duplication: of rules and licenses. *Trends in cell biology*, *17*(5), 215-221.

Godinho, S. A., Picone, R., Burute, M., Dagher, R., Su, Y., Leung, C. T., ... & Pellman, D. (2014). Oncogene-like induction of cellular invasion from centrosome amplification. *Nature*, *510*(7503), 167-171.

Fukasawa, K., Choi, T., Kuriyama, R., Rulong, S., & Woude, G. F. V. (1996). Abnormal centrosome amplification in the absence of p53. *Science*, *271*(5256), 1744-1747.

Wong, Y. L., Anzola, J. V., Davis, R. L., Yoon, M., Motamedi, A., Kroll, A., ... & Oegema, K. (2015). Reversible centriole depletion with an inhibitor of Polo-like kinase 4. *Science*, *348*(6239), 1155-1160.

Marteil, G., Guerrero, A., Vieira, A. F., De Almeida, B. P., Machado, P., Mendonça, S., ... & Bettencourt-Dias, M. (2018). Over-elongation of centrioles in cancer promotes centriole amplification and chromosome missegregation. *Nature communications*, *9*(1), 1-17.

Ganapathi Sankaran, D., Stemm-Wolf, A. J., & Pearson, C. G. (2019). CEP135 isoform dysregulation promotes centrosome amplification in breast cancer cells. *Molecular biology of the cell*, *30*(10), 1230-1244.

Adams, S. D., Csere, J., D'angelo, G., Carter, E. P., Romao, M., Arnandis, T., ... & Godinho, S. A. (2021). Centrosome amplification mediates small extracellular vesicle secretion via lysosome disruption. *Current Biology*, *31*(7), 1403-1416.

D'Assoro, A. B., Lingle, W. L., & Salisbury, J. L. (2002). Centrosome amplification and the

development of cancer. *Oncogene*, *21*(40), 6146-6153.

Fukasawa, K. (2005). Centrosome amplification, chromosome instability and cancer development. *Cancer letters*, *230*(1), 6-19.

Davoli, T., & de Lange, T. (2011). The causes and consequences of polyploidy in normal development and cancer. *Annual review of cell and developmental biology*, *27*, 585-610.

Holland, A. J., & Cleveland, D. W. (2009). Boveri revisited: chromosomal instability, aneuploidy and tumorigenesis. *Nature reviews Molecular cell biology*, *10*(7), 478-487.

Kleylein-Sohn, J., Westendorf, J., Le Clech, M., Habedanck, R., Stierhof, Y. D., & Nigg, E. A. (2007). Plk4-induced centriole biogenesis in human cells. *Developmental cell*, *13*(2), 190-202.

Kim, J., Kim, J., & Rhee, K. (2019). PCNT is critical for the association and conversion of centrioles to centrosomes during mitosis. *Journal of cell science*, *132*(6), jcs225789.

Jung, G. I., & Rhee, K. (2021). Triple deletion of TP53, PCNT, and CEP215 promotes centriole amplification in the M phase. *Cell Cycle*, *20*(15), 1500-1517.

Shin, B., Kim, M. S., Lee, Y., Jung, G. I., & Rhee, K. (2021). Generation and Fates of Supernumerary Centrioles in Dividing Cells. *Molecules and Cells*, *44*(10), 669.

Brodie, K. M., & Henderson, B. R. (2012). Characterization of BRCA1 protein targeting, dynamics, and function at the centrosome: a role for the nuclear export signal, CRM1, and Aurora A kinase. *Journal of Biological Chemistry*, *287*(10), 7701-7716.

Rhys, A. D., Monteiro, P., Smith, C., Vaghela, M., Arnandis, T., Kato, T., ... & Godinho, S. A. (2018). Loss of E-cadherin provides tolerance to centrosome amplification in epithelial cancer cells. *Journal of Cell Biology*, *217*(1), 195-209.

Gasparri, F., Ciavolella, A., & Galvani, A. (2007). Cell-cycle inhibitor profiling by high-content analysis. *Advances in Molecular Oncology*, 137-148.

Wang, G., Jiang, Q., & Zhang, C. (2014). The role of mitotic kinases in coupling the centrosome cycle with the assembly of the mitotic spindle. *Journal of cell science*, *127*(19), 4111-4122.

Shinmura, K., Kurabe, N., Goto, M., Yamada, H., Natsume, H., Konno, H., & Sugimura, H. (2014). PLK4 overexpression and its effect on centrosome regulation and chromosome stability in human gastric cancer. *Molecular biology reports*, *41*(10), 6635-6644.

Coelho, P. A., Bury, L., Shahbazi, M. N., Liakath-Ali, K., Tate, P. H., Wormald, S., ... & Glover, D. M. (2015). Over-expression of Plk4 induces centrosome amplification, loss of primary cilia and associated tissue hyperplasia in the mouse. *Open biology*, *5*(12), 150209.

Serçin, Ö., Larsimont, J. C., Karambelas, A. E., Marthiens, V., Moers, V., Boeckx, B., ... & Blanpain, C. (2016). Transient PLK4 overexpression accelerates tumorigenesis in p53-deficient epidermis. *Nature cell biology*, *18*(1), 100-110.

Kao, C. H., Su, T. Y., Huang, W. S., Lu, X. Y., Jane, W. N., Huang, C. Y., ... & Wang, W. J. (2022). TFEB-and TFE3-dependent autophagy activation supports cancer proliferation in the absence of centrosomes. *Autophagy*, 1-21.

Flanagan, A. M., Stavenschi, E., Basavaraju, S., Gaboriau, D., Hoey, D. A., & Morrison, C. G. (2017). Centriole splitting caused by loss of the centrosomal linker protein C-NAP1 reduces centriolar satellite density and impedes centrosome amplification. *Molecular biology of the cell*, *28*(6), 736-745.

Holland, A. J., Fachinetti, D., Zhu, Q., Bauer, M., Verma, I. M., Nigg, E. A., & Cleveland, D. W. (2012). The autoregulated instability of Polo-like kinase 4 limits centrosome duplication to once per

cell cycle. *Genes & development*, *26*(24), 2684-2689.

McPherson, J. P., Tamblyn, L., Elia, A., Migon, E., Shehabeldin, A., Matysiak-Zablocki, E., ... & Hakem, R. (2004). Lats2/Kpm is required for embryonic development, proliferation control and genomic integrity. *The EMBO journal*, *23*(18), 3677-3688.

Fujiwara, T., Bandi, M., Nitta, M., Ivanova, E. V., Bronson, R. T., & Pellman, D. (2005). Cytokinesis failure generating tetraploids promotes tumorigenesis in p53-null cells. *Nature*, *437*(7061), 1043-1047.

Nishio, M., Hamada, K., Kawahara, K., Sasaki, M., Noguchi, F., Chiba, S., ... & Suzuki, A. (2012). Cancer susceptibility and embryonic lethality in Mob1a/1b double-mutant mice. *The Journal of clinical investigation*, *122*(12), 4505-4518.

Sabino, D., Gogendeau, D., Gambarotto, D., Nano, M., Pennetier, C., Dingli, F., ... & Basto, R. (2015). Moesin is a major regulator of centrosome behavior in epithelial cells with extra centrosomes. *Current Biology*, *25*(7), 879-889.

국문 초록

중심체는 2개의 중심립과 중심구로 구성된 세포 내 소기관이다. 중심립의 복제 및 분리는 세포주기와 밀접하게 연관되어 있다. S 기에서 딸 중심립은 기존 존재하는 중심립의 끝부분에서 자라나고 유사분열이 끝나면 두 개의 중심립 쌍이 각 딸세포로 분리된다. 중심체 수는 엄격하게 조절되어야 하는데, 그렇지 않으면 비정상적인 방추체가 형성되어 유사분열문제와 이수성을 일으킨다. 그럼에도 불구하고 암세포는 종종 과량의 중심립을 포함한다. 본 연구는 암세포주에서 과량의 중심립이 어떻게 형성되는지 조사했다. 16개 암세포주에서 특정 세포 주기 단계의 중심체 수를 헤아리기 위해 순차적인 면역염색을 수행했다. 그 결과 MDA-MB-157, DU145, SKBR3 및 RD, 4개의 암세포주에서 중심립의 수가 G2 및 M기에서 유의미하게 증가되었다. 그러나 조사한 암세포주 중 S기 중심립 증폭은 검출하지 못했다. 또한 M 기 상에서 과량의 중심립을 갖는 MDA-MB-157 및 RD에서 M 기에서의 조숙한 중심립 유리현상을 관찰하였다. 이 결과를 바탕으로 특정 암세포주에서 M기 중심립 증폭이 발생할 수 있음을 제안한다.

주요어: 과량의 중심립, 중심립, 중심체, 중심립 유리현상, 중심구, 암